Application of nonlinear methods to discriminate fractionated electrograms in paroxysmal versus persistent atrial fibrillation

ACHARYA, U.R., FAUST, Oliver <http://orcid.org/0000-0002-0352-6716>, CIACCIO, E.J., KOH, J.E.W., OH, S.L., TAN, R.S. and GARAN, H.

Application of nonlinear methods to discriminate fractionated electrograms in paroxysmal versus persistent atrial fibrillation

U. Rajendra Acharya[1,2,3], Oliver Faust[4*], Edward J. Ciaccio[5], Joel Koh En Wei[1], Oh Shu Lih[1], Tan Ru San[6] and Hasan Garan[5]

[1]*Department of Electronic & Computer Engineering, Ngee Ann Polytechnic, Singapore*
[2]*Department of Biomedical Engineering, School of Science and Technology, SIM University, Singapore* [3]*Department of Biomedical Imaging, Faculty of Medicine, University of Malaya, Kuala Lumpur, Malaysia*
[4]*Department of engineering and mathematics, Sheffield Hallam University, Sheffield UK*
[5] *Department of Medicine - Division of Cardiology, Columbia University, New York, USA*
[6]*National Heart Centre Singapore, Singapore*
*Corresponding author:
Postal Address: Department of engineering and mathematics, Sheffield Hallam University, Sheffield UK
Telephone: +44 225 6700; Email Address: oliver.faust@gmail.com

Abstract

Background and Objective: Complex fractionated atrial electrograms (CFAE) may contain information concerning the electrophysiological substrate of atrial fibrillation (AF); therefore they are of interest to guide catheter ablation treatment of AF. Electrogram signals are shaped by activation events, which are dynamical in nature. This makes it difficult to establish those signal properties that can provide insight into the ablation site location. Nonlinear measures may improve information. To test this hypothesis, we used nonlinear measures to analyze CFAE.

Methods: CFAE from several atrial sites, recorded for a duration of 16 seconds, were acquired from 10 patients with persistent and 9 patients with paroxysmal AF. These signals were appraised using non-overlapping windows of 1-, 2- and 4-second durations. The resulting data sets were analyzed with Recurrence Plots (RP) and Recurrence Quantification Analysis (RQA) . The data was also quantified via entropy measures.

Results: RQA exhibited unique plots for persistent versus paroxysmal AF. Similar patterns were observed to be repeated throughout the RPs. Trends were consistent for signal segments of 1 and 2 seconds as well as 4 seconds in duration. This was suggestive that the underlying signal generation process is also repetitive, and that repetitiveness can be detected even in 1-second

sequences. The results also showed that most entropy metrics exhibited higher measurement values (closer to equilibrium) for persistent AF data. It was also found that Determinism (DET), Trapping Time (TT), and Modified Multiscale Entropy (MMSE), extracted from signals that were acquired from locations at the posterior atrial free wall, are highly discriminative of persistent versus paroxysmal AF data.

Conclusions: Short data sequences are sufficient to provide information to discern persistent versus paroxysmal AF data with a significant difference, and can be useful to detect repeating patterns of atrial activation.

Keywords: Electrogram; Recurrence plot; Recurrence quantification analysis; Entropy measures.

1. Introduction

Atrial fibrillation (AF) is a common arrhythmia that occurs in approximately 1–2% of the population worldwide (Stewart et al., 2001) especially among the elderly (Go et al., 2001). There are three clinical patterns of AF: paroxysmal, in which the arrhythmia occurs and terminates spontaneously; persistent, where AF duration is greater than an arbitrarily defined period of 7 days and rarely terminates without pharmacological or electrical cardioversion (Go et al., 2001); and permanent, where the arrhythmia does not terminate by any known means. Irrespective of type, AF increases the risk of thromboembolic stroke five-fold (Flegel et al., 1987), which has motivated therapeutic efforts to mitigate the thromboembolic risk with antithrombotic drugs (AF Investigators, 1994) and/or to eliminate AF definitively.

Since the discovery of spontaneous AF initiation from ectopic foci originating at the pulmonary vein ostia (Haïssaguerre et al., 1998), pulmonary vein antrum isolation (PVAI) with radiofrequency catheter ablation (RFCA) has become the mainstay for curative treatment of AF, with long-term success being observed in some patients. Mapping of the atrial electrophysiologic substrate to guide adjuvant catheter ablation of atrial regions, identified to

have complex fractionated atrial electrograms (CFAE), has been demonstrated in some studies to improve the success of AF termination without recurrence, as compared with anatomically based pulmonary vein antrum isolation (PVAI) ± linear ablation (Willems et al., 2006; Oral et al., 2009). It has been postulated that CFAE represent local sites for reentry, instrumental in perpetuating AF (Nademanee et al., 2004). In published clinical trials, the long-term results for successful maintenance of sinus rhythm after PVAI + CFAE ablation has been mixed (Li et al., 2011; Providência et al., 2015), particularly for paroxysmal AF, which responds well to standard PVAI alone (Li et al., 2011). Important limitations of a CFAE approach targeting nonparoxysmal AF include: the wide heterogeneity among patients with persistent AF (recent-onset persistent AF plausibly shares more electrophysiological substrate similarity with paroxysmal AF than long-standing persistent AF); the lack of standardized criteria for CFAE among studies; and the substantial time demands of substrate mapping. In order to characterize substrate differences in paroxysmal versus persistent types of AF, it would be helpful to devise a fast, accurate and reproducible CFAE measurement that can efficiently characterize electrogram differences. This might also be useful to stratify patients for adjuvant CFAE ablation. We hypothesized that advanced computational analysis of electrogram features could be highly discriminative for this purpose.

The electrogram waveform is comprised of several deflections caused by unsynchronized electrical activation events that appear as low amplitude noise (Latchamsetty and Morady, 2011). These signals provide information about the AF complexity, and one way to extract this information is to measure the amount of repetitiveness in the waveforms (Ciaccio et al., 2011, 2012). That repetitiveness is defined in the fractal sense, which indicates that similar electrogram shapes repeatedly occur at different time epochs. The interval between these epochs may differ, i.e. there is no clear rhythm (Ciaccio et al., 2011, 2012). More repetitiveness implies that the underlying electrical activation patterns are more reproducible (Faust and Bairy, 2012).

In this study, we used a novel method of signal analysis applied to data previously used in other of our published works (Ciaccio et al., 2011, 2012) to

confirm the prior results with a different technique. Recently, recurrence quantification analysis (RQA) has been used for the detection of AF(Zeemering et al., 2015; Hummel et al, 2017; Almeida et al, 2018). The following sections detail the study setup, including the data acquisition mode and analysis methods; study results including RPs and bar plots for the means and variances of the RQA features; discussion and interpretation including practical application; and conclusion.

2. Materials and methods

Herein, we used Recurrence Plots (RPs) to quantify the repetitiveness of CFAE measured during RFCA in patients with either paroxysmal or long-standing persistent AF. These plots were generated from 1-, 2-, and 4-second signal segments with a threshold value = 0.1. Visual inspection indicated that there were distinct RPs for paroxysmal versus persistent data in 1-, 2-, and 4-second segments. The differences were quantified using four RQA measures and four entropy measures. The block diagram, shown in Figure 1 details the study setup. We have structured the work into the following steps: data acquisition, signal preprocessing, RP plot generation, quantification, and statistical analysis of entropy and RQA measures. The next sections introduce these steps in detail.

2.1 Data used

Data were obtained from consecutive patients with paroxysmal (n=9) and long-standing persistent AF (n=10) who underwent RFCA at the cardiac electrophysiology laboratory of Columbia University Medical Center. Electrograms were recorded for 16 s at 977 Hz at each of the following locations: the left pulmonary vein ostia —LSPV, left inferior pulmonary vein (LIPV), right superior pulmonary vein (RSPV) and right inferior pulmonary vein (RIPV)— and free wall sites at the anterior (ANT) and posterior (POS) left atrial free wall. CFAE were identified as having multiple deflections and varying patterns, with a maximum average interval of 50 milliseconds between

deflections, based on published criteria (Ciaccio et al., 2013). One hundred and fourteen and 90 CFAE persistent and paroxysmal AF patient data, respectively, were analyzed. These signals were subjected to a rectangular windowing function that yielded three distinct datasets. The first dataset consisted of 204 non-overlapping 1-second sequences. The second, consisted of 204 non-overlapping 2-second sequences and the third consisted of 204 non-overlapping 4-second sequences.

The Internal Review Board (IRB) at Columbia University Medical Center approved acquisition and analysis of these retrospective data. All patients had either paroxysmal or long-standing persistent AF, were not on arrhythmogenic drug therapy, and were undergoing radiofrequency catheter ablation for treatment of AF. In paroxysmal AF patients with a baseline sinus rhythm, AF was induced by rapid pacing at the coronary sinus or at the lateral wall of the right atrium (coupling interval range 250 to 200 ms). AF was required to persist for greater than 10 minutes for the electrogram to be included for analysis. Signals were filtered with a bandpass by the acquisition system prior to discretization, which removed baseline drift and high frequency noise (CardioLab, GE Healthcare, Waukesha, WI). The 977 Hz sampling rate corresponded to approximately 1 millisecond intervals between discrete time samples. Signal amplitudes were measured in millivolts.

2.2 Recurrence plot

RPs provide a visual representation of the way in which an observed system behaves in phase space (Eckmann et al., 1987). For image analysis, we assigned a value of one to each black dot, and zero to each white dot. The resultant two-dimensional matrix is depicted as a RP, where each dot corresponds to a matrix element. The real-valued matrix elements that represent vector distances are depicted in color. Hence, most RPs are two-dimensional color-coded plots that can be used to reconstruct the time series (Bakeman and Quera, 2011). Figure 2 shows an example RP, which illustrates qualitatively the RQA measures that were used in this study. To quantify the RQA and entropy measures objectively, it was necessary to introduce a common threshold for all matrix elements. That

threshold converts the matrix with real-valued elements into a binary matrix. Figures 3 and 4 show such a binary or thresholded RP for electrogram signals. In this work, we have set the threshold value of 0.1 to have more lines and clear separation between the two classes for three durations (1, 2 and 4 seconds).

2.3 Entropy measures

From the RP, we extracted signatures in the form of features. The first group of features characterizes the entropy from the way in which the line segments are distributed. The line segments result from the state-space trajectories, and such measures are useful to quantify both the number and duration of recurrences in a dynamical system, such as the human heart. The second group of features, RQA measures, establish the hidden repetition of waveform shapes in the signal. These measures characterize both nonlinearity and complexity in time series signals (Zbilut and Webber Jr, 1992).

Fuzzy Entropy (FEn) is based on the idea of a fuzzy set whose elements are permitted to have different levels of membership. The level of membership captures the randomness, and the method provides a way to establish the entropy, which measures the information content (Kosko, 1986). Sample Entropy (SampEn) measures the information contained in the regularity of a physiological signal. The results are largely independent of sequence length, i.e. SampEn measures are consistent regardless of sequence length if the signal statistics are stationary. This is advantageous particularly when shorter sequences are analyzed. Compared with other measures, such as approximate entropy, SampEn has less bias (Richman and Moorman, 2000). A low SampEn value indicates that there is less information in the signal waveform, implying that the signal, and the underlying process, is more predictable. In contrast, if the signal is unpredictable, its information content and the SampEn value are high.

Multiscale Entropy (MSE) characterizes the complexity of a finite time series. In contrast to conventional entropy algorithms that assume a linear relationship between complexity and information, the MSE algorithm employs a coarse-graining procedure that reduces the time series length. When applied to a short sequence, the MSE algorithm may yield an imprecise estimation of, or even an

undefined, entropy, which is problematic. The Modified Multiscale Entropy (MMSE) algorithm (Costa et al., 2002) mitigates this dilemma by replacing the coarse-graining with a moving-average procedure. Furthermore, template vectors are calculated using time delays when the sample entropy is constructed. MMSE algorithms can better quantify the complexity of time series for a range of scales, and they are more reliable than standard MSE algorithms for short-term time series analysis (Wu et al., 2013).

Diagonal Line Lengths Entropy (DLLE) measures complexity based on the variation of diagonal lines in RPs. The diagonal line length is an indicator of the divergence of trajectory segments: a diagonal line length close to unity means that a segment of the trajectory at one time step is close to another segment of the trajectory at a different time step. For our work, we fixed the minimal diagonal line length as $l_{min} = 2$, as electrogram data can be noisy, and a larger l_{min} is required for smoother continuous data (Marwan et al., 2002).

2.4 Recurrence quantification analysis (RQA) measures

Determinism (DET) captures the predictability of a dynamical system by measuring the percentage of recurrence points that belong to diagonal lines of a minimum length, i.e. $l_{min} = 2$. It is predicated on the premise that a RP from white noise possesses numerous diagonal lines but sparse single dot features; hence noise-like signals have low DET values. Laminarity (LAM), also known as intermittency, provides a similar measure for the number of recurrence points that form vertical lines, thereby quantifying the number of laminar phases in the system.

Trapping Time (TT) is related to LAM. The algorithm measures the average vertical line length, which is an indicator of the time that a system remains in a specific state. Hence, TT reflects how far into the future it is possible to predict a dynamical system, i.e. it quantifies the time during which a nonlinear system is predictable.

2.5 Statistical feature assessment

We used the 2-sample t-test to refute the null hypothesis that RQA and entropy features are similar for paroxysmal versus persistent AF. The algorithm establishes the ratio of the deviation of the estimated value of a parameter from its hypothesized value to its standard error (Box, 1981). A large t-test value provides strong support for rejection of the null hypothesis.

3. Results

Figure 3 depicts RPs from 1-, 2-, and 4-second segments of CFAE data obtained from the LSPV site measured from the anterior atrial free wall. Figure 4 shows the RPs from the same location measured at the posterior free wall. Visual inspection shows that the RPs, at the same measurement site from the same CFAE segment duration, are very different. The RPs for persistent AF exhibited denser square clusters compared with paroxysmal AF. The crowdedness of the squares was more prominent with 4- versus 2-second and 1-second data.

The statistical feature analysis for LSPV, LIPV, RSPV, RIPV, POS, and ANT are tabulated in Tables 1A, 2A, 3A, 4A, 5A and 6A, respectively, in Appendix A. These tables, as well as bar plots in Figures 5 to 10, demonstrate that SampEn, FEn, MMSE 1 and 2 generally showed higher —and DET, LAM, TT, DLLE, lower— values for persistent versus paroxysmal AF. This suggests that CFAE from patients with persistent AF are less ordered as compared with those from paroxysmal AF. A higher signal variability results in higher entropy values for SampEn, FEn, MMSE 1 and 2. In contrast, DET, LAM, TT, and DLLE were lower for persistent than for paroxysmal AF, because in persistent AF the trend repeats faster than for paroxysmal AF. Apart from these general trends, we also found that DLLE, TT, DET and LAM extracted from 1-second signal sequences measured at the POS highly discriminated paroxysmal from persistent AF, as shown in Figure 9 and Table 5A. Furthermore, MMSE 1, extracted from 4-second sequences measured at the LSPV antrum, highly discriminated paroxysmal from persistent AF, as shown in Figure 5 and Table 1A. Most of the p-values are highly significant in

discerning paroxysmal from persistent AF data, particularly for recordings acquired from the LSPV and Posterior regions. Regarding some of the details, generally the MMSE 1 mean value for paroxysmal data was lower than the mean value for persistent data, such that there was no overlap in the feature variances. Figures 11 and 12 show the f-value for the eight individual features extracted from the RP plots measured at six different locations. The first part of the feature name indicates the measurement location, i.e. ANT, LIP, POS, RIP and RSP[1]. The second part indicates the feature name, i.e. FEn, SampEn, MMSE 1 / 2, DLLE, DET, LAM, and TT. In both figures, the orange line represents the feature performance for 1 second signal segments. The green and blue lines represent the feature performance for 2 and 4 second signal segments respectively. Figure 11 shows the f-values for features measured at the posterior free wall. POS DLLE extracted from 1-second electrogram segments, located at 3 o'clock in the diagram, shown in Figure 11, has the largest t-value of all tested features (most significant). The f-values are decreasing counterclockwise. To be specific, the ordering was based on the f-value results for 1 second segments. Figure 12 shows the f-values for features measured at the anterior region of the heart. The feature order is the same as for the graph shown in Figure 11. The fact that the f-values do not decrease counterclockwise indicates that the feature performance is different for electrogram measurements from the anterior and posterior regions of the heart. Furthermore, the graphs in Figure 11 show that POS is a satisfactory location for comparison of AF types when 1-second segments are considered, in contrast to 4-second segments where the LSPV region yields better features.

In summary, long-standing persistent AF, as compared with paroxysmal AF, exhibited higher values for most entropy measures (and therefore is closer to the equilibrium state). Measurements from the LSPV were highly discriminative for persistent versus paroxysmal AF. The results were independent of sequence length analyzed (1- 2- and 4-second segments), demonstrating that the 1-second electrogram signals were of sufficient length to capture repetitiveness, and to discern between long-standing persistent and

[1] The V for vein was omitted for LSP(V), LIP(V), RSP(V), and RIP(V).

paroxysmal AF fractionated electrograms.

4. Discussion

In this study, using clinical data from prior work, but a different mode of analysis, confirmatory support is provided for our previously published results (Ciaccio et al., 2011, 2012). From visual inspection of Figures 3 and 4, the RPs derived from CFAE for persistent AF generally had more repetitiveness as compared with paroxysmal AF, for 1-, 2- and 4-second datasets. The repetitiveness was more intense for the 4- as compared to 2-second and 1-second data. We were able to use these RPs to discriminate the classes qualitatively. We also quantified the repetitiveness of CFAE using RQA and entropy measures derived from RPs, and 1-, 2- and 4-second datasets were subjected to the same analysis algorithms. The quantitative results in both test sets show that most entropies (apart from DLLE) have higher values, and DET, LAM, TT and DLLE have lower values, for persistent versus paroxysmal AF.

We thus established that RQA and entropy measures were useful to differentiate persistent from paroxysmal AF electrograms, and that the results were reproducibly independent of the segment length studied. The latter finding provides insight into the repetitiveness of CFAE, and shows that even 1-second segments can capture sufficient components of the repetitive process for detection, when using suitable nonlinear methods. This demonstration, and knowledge of the minimum required window length, has important implications for feature engineering, and for finding an initial set of hyperparameters that may be useful for deep learning in the quantitative analysis of fractionated AF electrograms.

Algorithm and its update

The results reported herein can be confirmed by testing a wide range of nonlinear analysis methods. We are particularly interested in features that

present with unique ranges for persistent versus paroxysmal AF. Having features with unique ranges is a first step toward construction of an automated AF discernment system, which might eventually be used to detect arrhythmogenic regions. Whether the patient is in a paroxysmal versus persistent AF state is evident upon their admission. Yet, analysis of fractionated electrogram morphology may be helpful to discern the severity of the paroxysmal or persistent state, analogous to determining the progress of the arrhythmia in terms of tissue remodeling, and could therefore be useful to devise an optimal ablation paradigm, and perhaps to estimate the likelihood of arrhythmia recurrence after ablation. Feature-based machine classification works well on a small volume of data, because it is possible to control the feature selection process, and thereby to control the information that is presented to the classifier. Despite the shortcomings of feature engineering, such a system should support our finding that it is feasible to automate the classification of CFAE into persistent and paroxysmal types, and perhaps to determine the degree of severity in each state. The identification of features of true longstanding persistent AF from CFAE may potentially improve the selection of patients or foci for substrate-based adjuvant RFCA, in addition to PVAI for AF.

This work justifies the collection of more diverse data, which can be used to design classification models with higher complexities. With these improved models, it would be possible to avoid feature engineering altogether, and input the raw data to the classification algorithm using deep learning (Faust et al., 2018b). Developing a classification method that can handle big data would be useful for eventually devising a diagnostic support system. Any such system could be based on the Internet of Medical Things technology, which incorporates a cloud server for data storage and review, as well as deep learning for real-time classification (Kareem and Faust, 2018), that is pertinent for intraprocedural annotation and decision-making. After recording, the electrogram signals would be stored in the cloud server, which would make them universally accessible. At the same time, deep learning might be used to select an optimal catheter ablation site. A medical practitioner could then

review the information and act on the suggestion by observing the CFAE signal analysis in real-time on the cloud server.

Limitations

We tested a small data volume. CFAE signals are dynamic, with wide inter-patient variability. Even in the same patient, different waveform characteristics may present at different times. More and longer signal segments would be needed to confirm that 1-second signal segments contain sufficient information concerning the repetitiveness of CFAE. Furthermore, these canonical sites of data collection ignore substantial areas of the left atrium, and the entire right atrium. The omitted sites can harbor abnormal electrophysiologic parameters, which may be contributing to the underlying mechanism of AF. Another issue is the fact that RQA and entropy measures extract specific information that constitutes only a small subset of the available information. In fact, feature extraction methods, such as RQA, inherently involve processes for information reduction, which reduces the quantity of information available for discrimination. Feature engineering leads to information reduction and information duplication that may ultimately reduce diagnostic quality (Faust et al., 2018a). The problem is magnified when moving from the research environment to the design of practical diagnostic support systems.

5. Conclusion

Persistent and paroxysmal AF CFAE signals of 1-, 2-, and 4-second duration were analyzed using nonlinear features, namely RQA and various entropies. Our results show that most entropies (SampEn, FEn, MMSE 1 and 2) had higher values for persistent as compared to paroxysmal AF. This may be because persistent AF signals are highly varying compared with paroxysmal AF. More variability resulted in higher entropies. Also, our findings indicate that DET, LAM, TT and DLLE were lower for persistent than paroxysmal AF data, which may also be due to higher variation in the persistent AF electrogram morphology.

Furthermore, the RPs from persistent AF CFAE have more repeating

features when compared to those from paroxysmal AF CFAE for 1-, 2-, and 4-second segments. Also, this regularity is more intense for 4-second as compared with the 2- and 1-second data. Hence, we can use these RPs to discern between the two classes.

This work establishes that when using even a short 1-second interval of CFAE data, it is possible to discriminate the two classes using nonlinear features and RPs. In the future, we intend to obtain more data, and use the features to further characterize fractionated electrograms, possibly also to estimate the degree of severity within each arrhythmia type.

Acknowledgement: We thank Angelo B. Biviano, MD, Columbia University, for kindly acquiring and sharing the clinical atrial fibrillation data used in this study.

Acronyms

AF	Atrial Fibrillation
ANT	Anterior left atrial free wall
DET	Determinism
DLLE	Diagonal Line Lengths Entropy
FEn	Fuzzy Entropy
LA	Left Atrium
LAM	Laminarity
LIPV	Left Inferior Pulmonary Vein
LSPV	Left Superior Pulmonary Vein
MMSE	Modified Multiscale Entropy
MSE	Multiscale Entropy
POS	Posterior left atrial free wall
RIPV	Right Inferior Pulmonary Vein
RQA	Recurrence Quantification Analysis
RP	Recurrence Plot
RSP	Right Superior Pulmonary
SampEn	Sample Entropy
TT	Trapping Time

References

Almeida, T.P, Schlindwein, F.S, Salinet, J, Li, X, Chu, G.S, Tuan, J.H, Stafford, P.J, André Ng, G, and Soriano, D. C.(2018). Characterization of human persistent atrial fibrillation electrograms using recurrence quantification analysis., *Chaos*, 28(8): 085710.

Atrial Fibrillation Investigators. (1994). Risk factors for stroke and efficacy of antithrombotic therapy in atrial fibrillation: analysis of pooled data from five randomized controlled trials. *Arch Intern Med*, 154:1449–1457.

Bakeman, R., and Quera, V. (2011). Sequential analysis and observational methods for the behavioral sciences. Cambridge University Press.

Box, J. F. (1981). Gosset, fisher, and the t distribution. *The American Statistician*, 35(2):61–66.

Ciaccio, E. J., Biviano, A. B., and Garan, H. (2013). The dominant morphology of fractionated atrial electrograms has greater temporal stability in persistent as compared with paroxysmal atrial fibrillation. *Computers in biology and medicine*, 43(12):2127–2135.

Ciaccio, E. J., Biviano, A. B., Whang, W., and Garan, H. (2012). Identification of recurring patterns in fractionated atrial electrograms using new transform coefficients. *Biomedical engineering online*, 11(1):4.

Ciaccio, E. J., Biviano, A. B., Whang, W., Vest, J. A., Gambhir, A., Einstein, A. J., and Garan, H. (2011). Differences in repeating patterns of complex fractionated left atrial electrograms in longstanding persistent as compared with paroxysmal atrial fibrillation. *Circulation: Arrhythmia and Electrophysiology*, pages CIRCEP–110.

Costa, M., Goldberger, A. L., and Peng, C.-K. (2002). Multiscale entropy analysis of complex physiologic time series. *Physical review letters*, 89(6):068102.

Eckmann, J. P., Kamphorst, S. O., and Ruelle, D. (1987). Recurrence plots of dynamical systems. EPL (Europhysics Letters), 4(9), 973.

Faust, O. and Bairy, M. G. (2012). Nonlinear analysis of physiological signals: a review. *Journal of Mechanics in Medicine and Biology*, 12(04):1240015.

Faust, O., Hagiwara, Y., Hong, T. J., Lih, O. S., and Acharya, U. R. (2018a). Deep learning for healthcare applications based on physiological signals: a review. *Computer methods and programs in biomedicine*.

Faust, O., Shenfield, A., Kareem, M., San, T. R., Fujita, H., and Acharya, U. R. (2018b). Automated detection of atrial fibrillation using long short-term memory network with RR interval signals. *Computers in biology and medicine*.

Flegel, K. M., Shipley, M. J., and Rose, G. (1987). Risk of stroke in non-rheumatic atrial fibrillation. *The Lancet*, 329(8532):526–529.

Go, A. S., Hylek, E. M., Phillips, K. A., Chang, Y., Henault, L. E., Selby, J. V., and Singer, D. E. (2001). Prevalence of diagnosed atrial fibrillation in adults: national implications for rhythm management and stroke prevention: the anticoagulation and risk factors in atrial fibrillation (atria) study. *Jama*,

285(18):2370–2375.

Haïssaguerre M, Jaïs P, Shah DC, Takahashi A, Hocini M, Quiniou G, Garrigue S, Le Mouroux A, Le Métayer P, and Clémenty J. Spontaneous initiation of atrial fibrillation by ectopic beats originating in the pulmonary veins. *N Engl J Med.* 1998;339:659–666.

Hummel, J.P., Baher, A, Buck, B, Fanarjian, M, Webber, C.L, and Akar, J.G. (2017). A method for quantifying recurrent patterns of local wavefront direction during atrial fibrillation. *Comput Biol Med,* 89: 497–504.

Kareem, M. and Faust, O. (2018). Design and implementation of a wireless heart health monitoring system for stroke risk mitigation. 12(8):192.

Kosko, B. (1986). Fuzzy entropy and conditioning. *Information sciences*, 40(2):165–174.

Latchamsetty, R. and Morady, F. (2011). Complex fractionated atrial electrograms: A worthwhile target for ablation of atrial fibrillation? *Circulation. Arrhythmia and electrophysiology*, 4(2):117–118.

Li WJ, Bai YY, Zhang HY, Tang RB, Miao CL, Sang CH, Yin XD, Dong JZ, Ma CS. Additional ablation of complex fractionated atrial electrograms after pulmonary vein isolation in patients with atrial fibrillation: a meta-analysis. Circ Arrhythm Electrophysiol. 2011 Apr;4(2):143-8.

Marwan, N., Wessel, N., Meyerfeldt, U., Schirdewan, A., and Kurths, J. (2002). Recurrence-plot based measures of complexity and their application to heart-rate-variability data. *Physical review E*, 66(2):026702.

Nademanee, K., McKenzie, J., Kosar, E., Schwab, M., Sunsaneewitayakul, B., Vasavakul, T., Khunnawat, C., and Ngarmukos, T. (2004). A new approach for catheter ablation of atrial fibrillation: mapping of the electrophysiologic substrate. *Journal of the American College of Cardiology*, 43(11):2044–2053.

Oral, H., Chugh, A., Yoshida, K., Sarrazin, J. F., Kuhne, M., Crawford, T., Chalfoun, N., Wells, D., Boonyapisit, W., Veerareddy, S., et al. (2009). A randomized assessment of the incremental role of ablation of complex fractionated atrial electrograms after antral pulmonary vein isolation for long-lasting persistent atrial fibrillation. *Journal of the American College of Cardiology*, 53(9):782–789.

Providência R, Lambiase PD, Srinivasan N, Ganesh Babu G, Bronis K, Ahsan S, Khan FZ, Chow AW, Rowland E, Lowe M, Segal OR. Is There Still a Role for Complex Fractionated Atrial Electrogram Ablation in Addition to Pulmonary Vein Isolation in Patients With Paroxysmal and Persistent Atrial Fibrillation? Meta-Analysis of 1415 Patients. Circ Arrhythm Electrophysiol. 2015 Oct;8(5):1017-29.

Richman, J. S. and Moorman, J. R. (2000). Physiological time-series analysis using approximate entropy and sample entropy. *American Journal of Physiology-Heart and Circulatory Physiology*, 278(6):H2039–H2049.

Stewart, S., Hart, C., Hole, D., and McMurray, J. (2001). Population prevalence, incidence, and predictors of atrial fibrillation in the Renfrew/paisley study. *Heart*, 86(5):516–521.

Willems S, Klemm H, Rostock T, Brandstrup B, Ventura R, Steven D, Risius T, Lutomsky B, Meinertz T. Substrate modification combined with pulmonary vein isolation improves outcome of catheter ablation in patients with persistent atrial fibrillation: a

prospective randomized comparison. Eur Heart J. 2006;27:2871–2878.

Wu, S.-D., Wu, C.-W., Lee, K.-Y., and Lin, S.-G. (2013). Modified multiscale entropy for shortterm time series analysis. *Physica A: Statistical Mechanics and its Applications*, 392(23):5865– 5873.

Zbilut, J. P. and Webber Jr, C. L. (1992). Embeddings and delays as derived from quantification of recurrence plots. *Physics letters A*, 171(3-4):199–203.

Zeemering, S, Bonizzi, S.P., Maesen, B, Peeters, R, and Schotten, U. (2015). Recurrence quantification analysis applied to spatiotemporal pattern analysis in high-density mapping of human atrial fibrillation. Conf Proc IEEE Eng Med Biol Soc, vol. 2015, :7704–7707.

A Result tables

Table 1A: Statistical feature analysis results for LSPV. In the table, ante. and post. are short forms for anterior and posterior regions of the heart.

Feature	pos	t	Persistent Mean	Persistent SD	Paroxysmal Mean	Paroxysmal SD	p-Value	t-Value
Fen	ante.	1	0.641	0.199	0.468	0.156	0.0095	2.7574
		2	0.630	0.196	0.458	0.144	0.008	2.8265
		4	0.593	0.19	0.432	0.128	0.0086	2.7986
	post.	1	0.585	0.213	0.425	0.143	0.0185	2.4832
		2	0.582	0.197	0.454	0.142	0.0423	2.1151
		4	0.560	0.189	0.417	0.106	0.0133	2.6221
SampEn	ante.	1	0.796	0.132	0.600	0.170	0.0007	3.7699
		2	0.668	0.126	0.484	0.139	0.0003	4.0216
		4	0.633	0.148	0.466	0.119	0.0012	3.541
	post.	1	0.702	0.148	0.517	0.120	0.0004	3.9159
		2	0.687	0.135	0.498	0.118	0.0002	4.2763
		4	0.673	0.135	0.473	0.091	0	4.8969
MMSE 2	ante.	1	0.676	0.203	0.438	0.202	0.0018	3.4011
		2	0.624	0.194	0.374	0.181	0.0006	3.8319
		4	0.569	0.203	0.335	0.152	0.0008	3.6907
	post.	1	0.621	0.212	0.381	0.144	0.0007	3.7399
		2	0.624	0.188	0.369	0.142	0.0001	4.3405
		4	0.601	0.183	0.330	0.095	0	5.206
MMSE 1	ante.	1	0.640	0.188	0.362	0.185	0.0002	4.2988
		2	0.622	0.168	0.345	0.179	0.0001	4.6306
		4	0.581	0.188	0.320	0.151	0.0001	4.3577
	post.	1	0.668	0.195	0.368	0.144	0	4.9544
		2	0.656	0.183	0.346	0.158	0	5.1899
		4	0.625	0.169	0.316	0.124	0	5.9295
DLLE	ante.	1	0.351	0.086	0.570	0.205	0.0002	4.2016
		2	0.297	0.077	0.506	0.189	0.0001	4.3825
		4	0.374	0.130	0.593	0.189	0.0004	3.9967
	post.	1	0.376	0.124	0.608	0.184	0.0001	4.3775
		2	0.383	0.116	0.654	0.180	0	5.2885
		4	0.403	0.114	0.681	0.167	0	5.7333
DET	ante.	1	0.526	0.118	0.735	0.163	0.0001	4.3302
		2	0.500	0.124	0.721	0.154	0.0001	4.632
		4	0.559	0.157	0.776	0.148	0.0003	4.0937
	post.	1	0.500	0.155	0.724	0.146	0.0002	4.2742
		2	0.516	0.150	0.762	0.145	0	4.8119
		4	0.535	0.143	0.789	0.122	0	5.4816
LAM	ante.	1	0.636	0.115	0.816	0.124	0.0001	4.352
		2	0.619	0.131	0.810	0.114	0.0001	4.4561
		4	0.663	0.150	0.848	0.106	0.0003	4.0404
	post.	1	0.607	0.151	0.816	0.107	0.0001	4.517
		2	0.622	0.152	0.844	0.115	0.0001	4.6678
		4	0.645	0.146	0.868	0.093	0	5.1366
TT	ante.	1	0.279	0.036	0.439	0.209	0.0027	3.2583
		2	0.191	0.024	0.322	0.202	0.0085	2.8049
		4	0.296	0.078	0.447	0.190	0.0035	3.1559
	post.	1	0.394	0.067	0.566	0.182	0.0006	3.8043
		2	0.402	0.058	0.604	0.170	0	4.8369
		4	0.414	0.057	0.624	0.169	0	5.0577

Table 2A: Statistical feature analysis results for LIPV.

Feature	pos	*t*	Persistent		Paroxysmal		*p*-Value	*t*-Value
			Mean	SD	Mean	SD		
FEn	ante.	1	0.5701	0.2685	0.4126	0.1592	0.0534	2.0058
		2	0.5513	0.2597	0.4007	0.1378	0.0509	2.0285
		4	0.5887	0.2732	0.441	0.1247	0.0617	1.9365
	post.	1	0.5722	0.2248	0.4211	0.1405	0.03	2.2714
		2	0.5887	0.2434	0.4361	0.1038	0.0304	2.265
		4	0.6282	0.2565	0.495	0.0885	0.0641	1.9181
SampEn	ante.	1	0.5863	0.216	0.5271	0.1219	0.3502	0.9481
		2	0.5842	0.2283	0.5378	0.1058	0.4732	0.7258
		4	0.628	0.2135	0.5596	0.1101	0.2684	1.1264
	post.	1	0.5962	0.1917	0.4782	0.1449	0.0566	1.9777
		2	0.5746	0.1863	0.4622	0.125	0.0536	2.004
		4	0.5674	0.1847	0.4607	0.1081	0.0563	1.9809
MMSE 2	ante.	1	0.4662	0.2649	0.3416	0.1256	0.1036	1.6752
		2	0.4753	0.2734	0.3539	0.1111	0.1166	1.613
		4	0.5169	0.2827	0.3847	0.1277	0.1034	1.6764
	post.	1	0.5788	0.2604	0.3749	0.1696	0.0133	2.6214
		2	0.5673	0.2644	0.3625	0.1684	0.0138	2.6065
		4	0.5528	0.2609	0.3814	0.1715	0.0356	2.194
MMSE 1	ante.	1	0.441	0.2352	0.3289	0.1418	0.1141	1.6244
		2	0.4653	0.253	0.3573	0.1356	0.1462	1.4895
		4	0.5066	0.2625	0.376	0.1503	0.0963	1.7134
	post.	1	0.5396	0.2561	0.329	0.1567	0.0087	2.7932
		2	0.5237	0.2473	0.3302	0.1749	0.0153	2.5626
		4	0.5172	0.2482	0.3382	0.1594	0.0212	2.4226
DLLE	ante.	1	0.5074	0.2078	0.5868	0.1865	0.256	1.1567
		2	0.4882	0.2207	0.5552	0.1559	0.3279	0.9936
		4	0.4883	0.2161	0.5654	0.1546	0.2526	1.165
	post.	1	0.3835	0.1608	0.5455	0.1943	0.0121	2.6606
		2	0.4289	0.1881	0.6018	0.2047	0.0154	2.5607
		4	0.4466	0.1896	0.6055	0.1922	0.0217	2.4127
DET	ante.	1	0.6384	0.2176	0.7192	0.1703	0.2468	1.1797
		2	0.5918	0.2092	0.6783	0.1404	0.1791	1.3736
		4	0.5928	0.2053	0.685	0.1343	0.143	1.5018
	post.	1	0.5377	0.1946	0.6955	0.1517	0.0147	2.58
		2	0.5665	0.2117	0.7257	0.1674	0.0234	2.3807
		4	0.5616	0.2086	0.7092	0.1521	0.0283	2.2979
LAM	ante.	1	0.726	0.1892	0.8056	0.1332	0.1771	1.3802
		2	0.6977	0.1855	0.7871	0.1104	0.1097	1.6455
		4	0.6992	0.1819	0.7933	0.107	0.0857	1.7733
	post.	1	0.6488	0.1924	0.7995	0.11	0.011	2.7
		2	0.6679	0.2017	0.8182	0.1354	0.0188	2.4749
		4	0.6677	0.1999	0.8092	0.126	0.0229	2.3892
TT	ante.	1	0.4783	0.1472	0.5314	0.1662	0.3316	0.986
		2	0.4047	0.1809	0.4201	0.1094	0.773	0.2909
		4	0.4222	0.1777	0.4485	0.1112	0.6205	0.5
	post.	1	0.3257	0.0855	0.4433	0.1989	0.0265	2.326
		2	0.4002	0.1135	0.5304	0.1969	0.0212	2.4227
		4	0.4354	0.1156	0.5541	0.1793	0.0257	2.3398

Table 3A: Statistical feature analysis results for RSPV.

Feature	pos	*t*	Persistent		Paroxysmal		*p*-Value	*t*-Value
			Mean	SD	Mean	SD		
FEn	ante.	1	0.6389	0.2328	0.3605	0.1532	0.0004	3.9931
		2	0.6157	0.2406	0.3641	0.1577	0.0014	3.4942
		4	0.6282	0.2358	0.3817	0.1561	0.0014	3.4861
	post.	1	0.5688	0.2164	0.3795	0.172	0.0094	2.7649
		2	0.6079	0.2247	0.3916	0.1675	0.004	3.1044
		4	0.6119	0.2285	0.3983	0.1628	0.0045	3.056
SampEn	ante.	1	0.6627	0.1668	0.5026	0.1956	0.0149	2.5745
		2	0.6571	0.1669	0.4947	0.18	0.0104	2.7224
		4	0.6754	0.1788	0.5095	0.1679	0.0095	2.7584
	post.	1	0.6669	0.2	0.5734	0.2099	0.1946	1.3248
		2	0.7038	0.1964	0.6065	0.2035	0.1672	1.4135
		4	0.5508	0.1736	0.4628	0.14	0.1208	1.5939
MMSE 2	ante.	1	0.6721	0.2434	0.4032	0.2452	0.0032	3.1885
		2	0.6641	0.2368	0.3997	0.233	0.0027	3.2556
		4	0.6221	0.2313	0.3736	0.1984	0.0023	3.3081
	post.	1	0.5529	0.2469	0.4062	0.2288	0.0852	1.7762
		2	0.5953	0.255	0.4413	0.2244	0.0748	1.8417
		4	0.5226	0.2288	0.3746	0.1833	0.0497	2.0399
MMSE 1	ante.	1	0.6451	0.2292	0.4053	0.2648	0.008	2.8285
		2	0.6517	0.2249	0.395	0.2388	0.003	3.2163
		4	0.62	0.2322	0.3855	0.2235	0.0056	2.9721
	post.	1	0.5252	0.2358	0.3953	0.2181	0.1092	1.6477
		2	0.5146	0.2259	0.4082	0.2184	0.1759	1.384
		4	0.5047	0.2119	0.3836	0.2072	0.1045	1.6708
DLLE	ante.	1	0.3501	0.1396	0.5531	0.2614	0.0066	2.9082
		2	0.3873	0.1655	0.5987	0.2506	0.0058	2.9566
		4	0.3623	0.1796	0.5285	0.1937	0.0144	2.5891
	post.	1	0.3773	0.1916	0.453	0.1795	0.2486	1.1751
		2	0.3683	0.1811	0.433	0.17	0.2959	1.0627
		4	0.4006	0.1822	0.4992	0.1884	0.1327	1.5429
DET	ante.	1	0.484	0.1566	0.6775	0.2287	0.0063	2.9247
		2	0.5086	0.1679	0.709	0.2123	0.0043	3.0759
		4	0.5094	0.1718	0.6901	0.1824	0.0057	2.9639
	post.	1	0.5264	0.1883	0.6193	0.1972	0.1714	1.3992
		2	0.536	0.1751	0.6184	0.1858	0.1946	1.3248
		4	0.5536	0.1874	0.6617	0.1812	0.1001	1.6936
LAM	ante.	1	0.6001	0.1512	0.7643	0.1914	0.0086	2.7979
		2	0.6248	0.1552	0.7959	0.1685	0.0043	3.0716
		4	0.6266	0.1554	0.7863	0.1466	0.0046	3.0482
	post.	1	0.6422	0.1646	0.7195	0.1787	0.1997	1.3096
		2	0.6553	0.1541	0.7229	0.166	0.2289	1.2265
		4	0.6656	0.1754	0.7606	0.1544	0.1087	1.6503
TT	ante.	1	0.3185	0.0895	0.4783	0.2433	0.0123	2.6542
		2	0.3782	0.1402	0.5456	0.2353	0.0147	2.5806
		4	0.3093	0.1719	0.4067	0.1506	0.0929	1.7322
	post.	1	0.3117	0.1761	0.3391	0.1108	0.6026	0.5258
		2	0.2871	0.1775	0.3082	0.1034	0.6858	0.4083
		4	0.3396	0.167	0.3902	0.1354	0.3489	0.9506

Table 4A: Statistical feature analysis results for RIPV.

Feature	pos	*t*	Persistent		Paroxysmal		*p*-Value	*t*-Value
			Mean	SD	Mean	SD		
FEn	ante.	1	0.635	0.215	0.6619	0.1957	0.7091	0.3764
		2	0.6414	0.2322	0.6296	0.1775	0.8719	0.1626
		4	0.6079	0.23	0.5743	0.1693	0.6387	0.4741
	post.	1	0.558	0.1999	0.4875	0.2042	0.3192	1.0118
		2	0.544	0.2139	0.4935	0.1893	0.4775	0.7188
		4	0.5512	0.2181	0.4883	0.1836	0.3784	0.8933
SampEn	ante.	1	0.5663	0.1782	0.5228	0.1505	0.4556	0.7554
		2	0.6773	0.197	0.6421	0.167	0.5847	0.5521
		4	0.6759	0.1907	0.6194	0.1831	0.3899	0.8716
	post.	1	0.6252	0.2196	0.5055	0.1346	0.0735	1.8506
		2	0.6192	0.2098	0.5134	0.1542	0.1123	1.6329
		4	0.6221	0.1875	0.5109	0.1565	0.0744	1.8445
MMSE 2	ante.	1	0.5072	0.252	0.4595	0.1869	0.5451	0.6117
		2	0.4974	0.2599	0.4332	0.1617	0.4091	0.8365
		4	0.4924	0.2511	0.4052	0.1682	0.2574	1.1532
	post.	1	0.4571	0.2466	0.3201	0.1416	0.0647	1.9134
		2	0.4523	0.2395	0.3363	0.1524	0.1127	1.6308
		4	0.435	0.2255	0.3107	0.1401	0.0711	1.8668
MMSE 1	ante.	1	0.5319	0.2551	0.4158	0.1742	0.142	1.5057
		2	0.5581	0.2731	0.4311	0.1734	0.1271	1.5666
		4	0.5543	0.2752	0.4104	0.1734	0.0873	1.764
	post.	1	0.4673	0.2577	0.3034	0.1325	0.0325	2.2357
		2	0.4568	0.25	0.3115	0.1432	0.0537	2.0034
		4	0.4613	0.2383	0.3067	0.1471	0.0353	2.1986
DLLE	ante.	1	0.3994	0.1702	0.4776	0.1734	0.1964	1.3193
		2	0.3962	0.1605	0.477	0.1735	0.169	1.4071
		4	0.3841	0.1504	0.47	0.1829	0.1425	1.5037
	post.	1	0.4516	0.2268	0.5693	0.1635	0.1007	1.6905
		2	0.3786	0.1677	0.4808	0.1754	0.0933	1.7299
		4	0.3494	0.1347	0.4686	0.1769	0.0328	2.2311
DET	ante.	1	0.5895	0.1741	0.6656	0.1337	0.1719	1.3974
		2	0.5906	0.1774	0.6684	0.128	0.1626	1.4293
		4	0.5885	0.1713	0.6739	0.1453	0.1331	1.5414
	post.	1	0.5901	0.2215	0.7362	0.1285	0.0303	2.2664
		2	0.5648	0.1962	0.6793	0.1385	0.065	1.9113
		4	0.5606	0.1747	0.6909	0.1305	0.0222	2.4039
LAM	ante.	1	0.6961	0.1561	0.7781	0.0998	0.087	1.7655
		2	0.6978	0.1591	0.7808	0.0965	0.0853	1.7757
		4	0.6995	0.1569	0.7828	0.1105	0.0913	1.741
	post.	1	0.6851	0.202	0.8249	0.0994	0.0199	2.4517
		2	0.6677	0.1849	0.7821	0.1065	0.0409	2.1308
		4	0.6716	0.1706	0.7951	0.0988	0.0182	2.489
TT	ante.	1	0.2675	0.1134	0.321	0.1949	0.3235	1.0028
		2	0.2695	0.1006	0.3275	0.1937	0.2672	1.1291
		4	0.244	0.0872	0.3091	0.2005	0.2115	1.275
	post.	1	0.4204	0.1836	0.4831	0.1449	0.2875	1.0816
		2	0.2477	0.0887	0.316	0.1969	0.1856	1.3529
		4	0.1939	0.0588	0.2754	0.2065	0.11	1.6441

Table 5A: Statistical feature analysis results for POS.

Feature	pos	*t*	Persistent		Paroxysmal		*p*-Value	*t*-Value
			Mean	SD	Mean	SD		
FEn	ante.	1	0.5698	0.2252	0.4395	0.1541	0.0648	1.9126
		2	0.5445	0.2201	0.4046	0.1214	0.0346	2.2069
		4	0.5513	0.2522	0.4105	0.1335	0.0597	1.9526
	post.	1	0.6283	0.214	0.436	0.1143	0.0036	3.138
		2	0.6124	0.2113	0.443	0.1103	0.0084	2.8107
		4	0.5801	0.2225	0.4248	0.1137	0.0197	2.4562
SampEn	ante.	1	0.6722	0.2249	0.5069	0.1295	0.0165	2.5298
		2	0.6592	0.2194	0.4853	0.105	0.0082	2.8172
		4	0.6682	0.2362	0.5238	0.1263	0.0405	2.1356
	post.	1	0.7074	0.1453	0.4689	0.0999	0	5.4174
		2	0.7428	0.1536	0.5114	0.1029	0	5.0076
		4	0.7116	0.1517	0.5124	0.1186	0.0002	4.1733
MMSE 2	ante.	1	0.5598	0.2657	0.3302	0.1804	0.0074	2.8612
		2	0.5569	0.2557	0.3164	0.1439	0.0027	3.2528
		4	0.5416	0.2804	0.3285	0.1507	0.0124	2.6511
	post.	1	0.6218	0.2059	0.2909	0.1288	0	5.4345
		2	0.6411	0.2119	0.3137	0.1291	0	5.2532
		4	0.5937	0.2093	0.3214	0.1433	0.0001	4.2997
MMSE 1	ante.	1	0.5759	0.2954	0.2983	0.1534	0.0024	3.2981
		2	0.5926	0.2969	0.2971	0.1336	0.0011	3.5721
		4	0.5539	0.2997	0.3042	0.1477	0.0059	2.9502
	post.	1	0.5716	0.2405	0.2355	0.1092	0	5.0093
		2	0.5395	0.2191	0.2381	0.1072	0	4.8766
		4	0.6032	0.2331	0.2965	0.1439	0.0001	4.4607
DLLE	ante.	1	0.3731	0.1938	0.56	0.1882	0.008	2.8286
		2	0.3686	0.1946	0.5616	0.1782	0.0055	2.9794
		4	0.3811	0.1866	0.5547	0.1839	0.0107	2.7121
	post.	1	0.4066	0.1342	0.7636	0.1862	0	6.4971
		2	0.3599	0.1159	0.631	0.1688	0	5.5471
		4	0.3527	0.1186	0.5988	0.185	0	4.7097
DET	ante.	1	0.5344	0.2112	0.7217	0.1594	0.0076	2.8503
		2	0.5168	0.2093	0.7187	0.1395	0.003	3.2117
		4	0.5489	0.2221	0.7278	0.1495	0.0117	2.674
	post.	1	0.4867	0.1429	0.7897	0.1274	0	6.4344
		2	0.5332	0.1549	0.8062	0.1304	0	5.4635
		4	0.5252	0.158	0.771	0.1449	0.0001	4.669
LAM	ante.	1	0.6356	0.2013	0.8141	0.1216	0.0049	3.0201
		2	0.6228	0.2005	0.8188	0.1016	0.0016	3.4456
		4	0.6516	0.2079	0.8227	0.1118	0.0072	2.8697
	post.	1	0.599	0.157	0.864	0.0942	0	5.7582
		2	0.6393	0.154	0.8694	0.0929	0	5.0925
		4	0.6353	0.1602	0.8473	0.106	0.0001	4.4116
TT	ante.	1	0.2261	0.1157	0.3271	0.2012	0.075	1.8402
		2	0.2729	0.137	0.3836	0.192	0.0586	1.9614
		4	0.2834	0.1127	0.3966	0.1975	0.0433	2.1047
	post.	1	0.4355	0.0632	0.7121	0.1879	0	6.0203
		2	0.3115	0.0509	0.5062	0.1844	0.0001	4.4103
		4	0.2807	0.0495	0.4542	0.2005	0.0009	3.6461

Table 6A: Statistical feature analysis results for ANT.

Feature	pos	*t*	Persistent		Paroxysmal		*p*-Value	*t*-Value
			Mean	SD	Mean	SD		
FEn	ante.	1	0.6682	0.1942	0.5582	0.1672	0.0913	1.7409
		2	0.6629	0.1908	0.5623	0.1822	0.129	1.5584
		4	0.6326	0.2027	0.5431	0.1814	0.1902	1.3385
	post.	1	0.745	0.1947	0.6089	0.1824	0.0455	2.0812
		2	0.7042	0.2021	0.5743	0.1737	0.0566	1.9782
		4	0.6925	0.1965	0.5649	0.1734	0.0566	1.978
SampEn	ante.	1	0.7397	0.1591	0.6305	0.1632	0.0581	1.9653
		2	0.7375	0.1223	0.6161	0.181	0.0262	2.3308
		4	0.755	0.1553	0.6491	0.1666	0.0648	1.9128
	post.	1	0.4649	0.0667	0.4477	0.1792	0.701	0.3875
		2	0.7375	0.1223	0.6161	0.181	0.0262	2.3308
		4	0.7514	0.1364	0.6214	0.1712	0.0191	2.4674
MMSE 2	ante.	1	0.6557	0.231	0.4606	0.2173	0.0173	2.5101
		2	0.6335	0.2171	0.4584	0.2324	0.0305	2.2645
		4	0.611	0.2276	0.4689	0.2046	0.0679	1.8894
	post.	1	0.4393	0.1025	0.3733	0.2209	0.2556	1.1576
		2	0.6634	0.1859	0.4717	0.2298	0.0112	2.691
		4	0.6429	0.1866	0.4603	0.2359	0.0169	2.5217
MMSE 1	ante.	1	0.5478	0.1762	0.3851	0.2206	0.0227	2.3932
		2	0.5436	0.1829	0.3864	0.2306	0.0338	2.2183
		4	0.6081	0.2197	0.4414	0.219	0.0352	2.1998
	post.	1	0.3497	0.0758	0.2994	0.2287	0.3738	0.9021
		2	0.6134	0.1614	0.4182	0.2177	0.0051	3.0046
		4	0.585	0.1707	0.4004	0.2312	0.0115	2.6797
DLLE	ante.	1	0.3875	0.1148	0.5217	0.1808	0.0128	2.6377
		2	0.3868	0.1163	0.5273	0.1933	0.013	2.6295
		4	0.4088	0.13	0.5322	0.1776	0.0257	2.3396
	post.	1	0.4735	0.0808	0.6076	0.2252	0.0216	2.4147
		2	0.4432	0.088	0.612	0.1858	0.0014	3.5035
		4	0.4244	0.1048	0.5982	0.1865	0.0016	3.4389
DET	ante.	1	0.5922	0.1417	0.7109	0.1482	0.0236	2.3773
		2	0.6003	0.1452	0.7211	0.1708	0.033	2.229
		4	0.5933	0.1506	0.7032	0.1512	0.0428	2.1093
	post.	1	0.5843	0.0914	0.7012	0.2183	0.042	2.1187
		2	0.5592	0.1025	0.7087	0.1573	0.0021	3.345
		4	0.5774	0.116	0.7338	0.1548	0.002	3.3712
LAM	ante.	1	0.7157	0.118	0.809	0.1218	0.031	2.2571
		2	0.7211	0.1189	0.815	0.141	0.043	2.1072
		4	0.7193	0.123	0.8096	0.1211	0.04	2.1406
	post.	1	0.7118	0.0826	0.7889	0.2171	0.1628	1.4285
		2	0.6969	0.0963	0.8154	0.1289	0.0043	3.0717
		4	0.7096	0.1012	0.8319	0.125	0.0035	3.1546
TT	ante.	1	0.2598	0.0775	0.3618	0.1926	0.0429	2.1085
		2	0.2504	0.0673	0.3583	0.197	0.0325	2.2352
		4	0.2695	0.0743	0.3602	0.1889	0.0638	1.9197
	post.	1	0.4753	0.0464	0.5966	0.1743	0.0064	2.9166
		2	0.4292	0.0506	0.5685	0.1699	0.0018	3.3993
		4	0.3683	0.0662	0.5083	0.1796	0.0035	3.1487

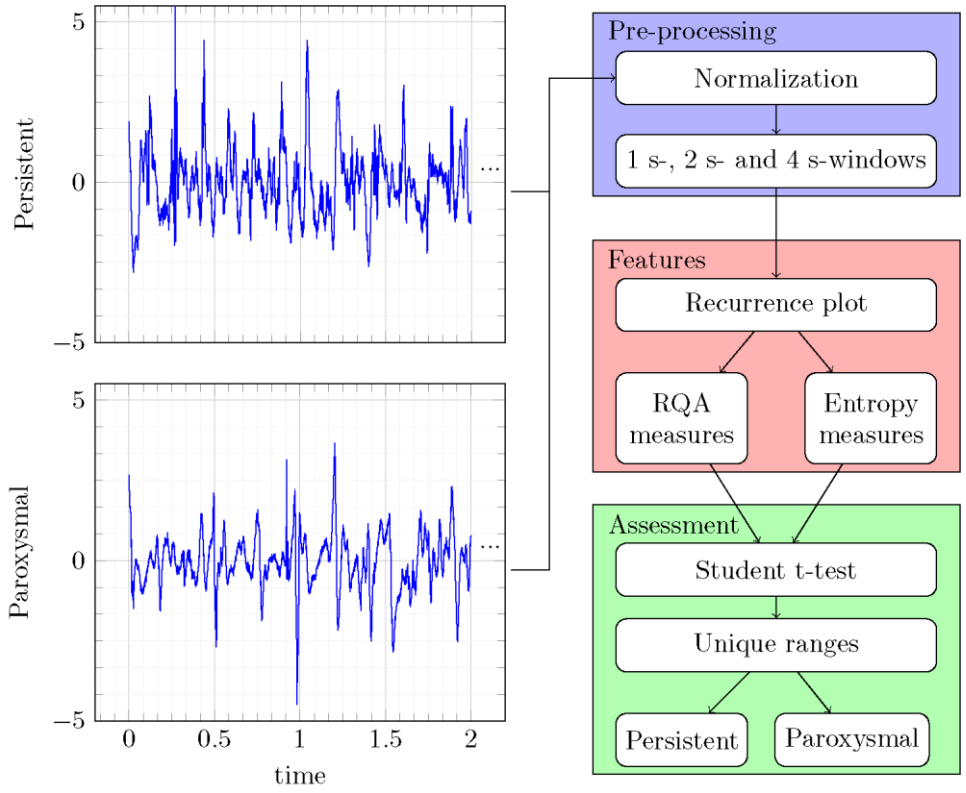

Figure 1: Block diagram of the proposed system. The electrogram signals on the left side show the first 2 seconds of 16-second sequences. The signals were measured at the left superior pulmonary vein ostia from patients with persistent and paroxysmal AF, respectively. These signals constitute the data for pre-processing and feature extraction algorithms. Feature extraction results were assessed with statistical methods, and features were identified that show unique ranges for persistent versus paroxysmal AF.

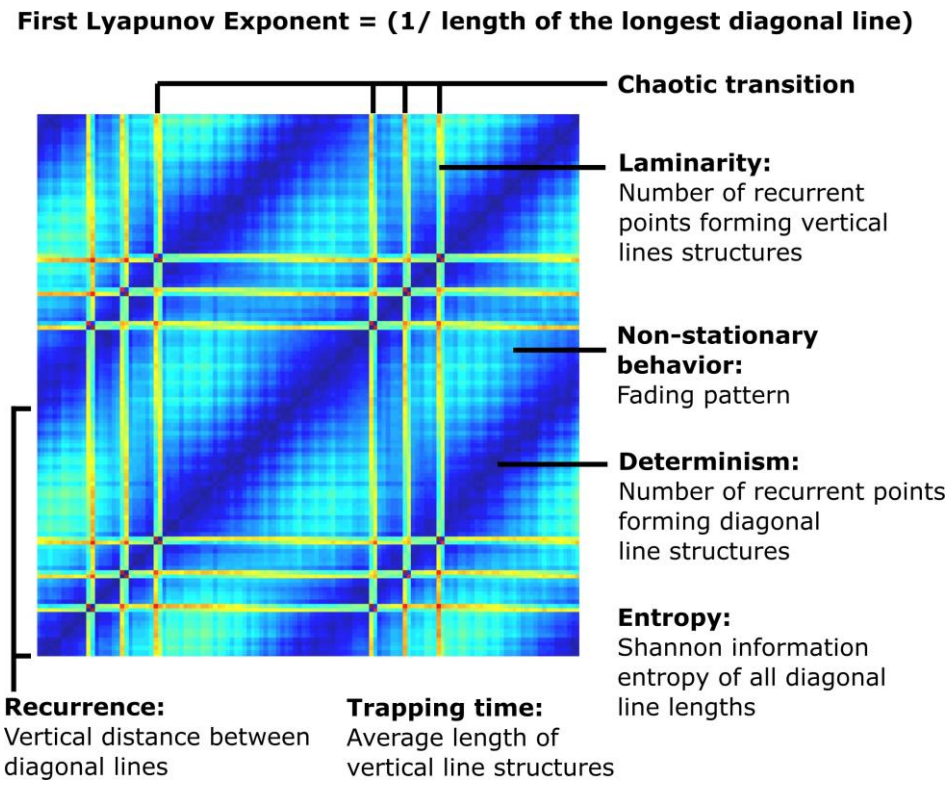

Figure 2: Sample RP with annotations that show RQA feature definitions.

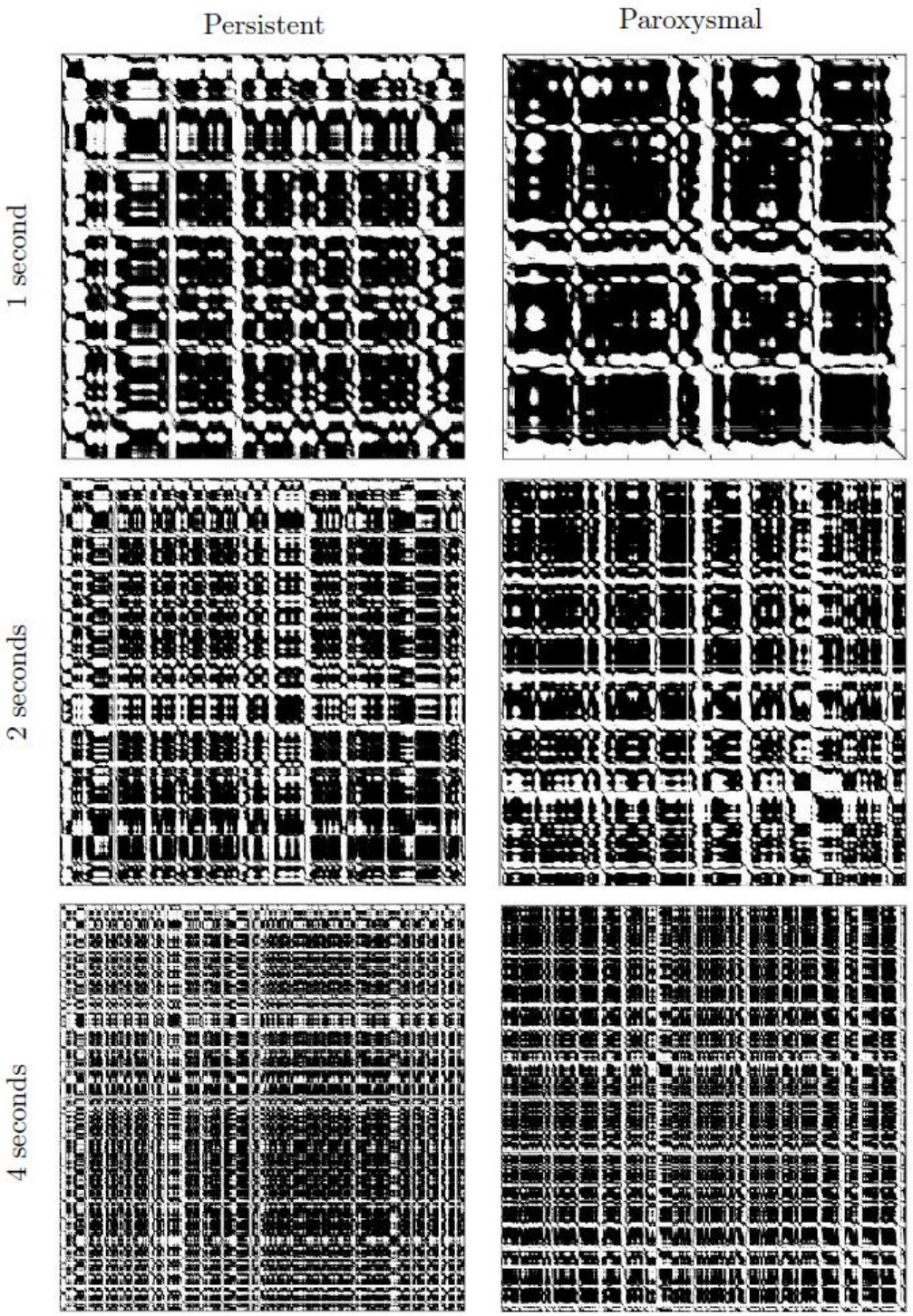

Figure 3: RPs from 1, 2 and 4 second segments measured from the left superior pulmonary vein ostia at the anterior region of the heart.

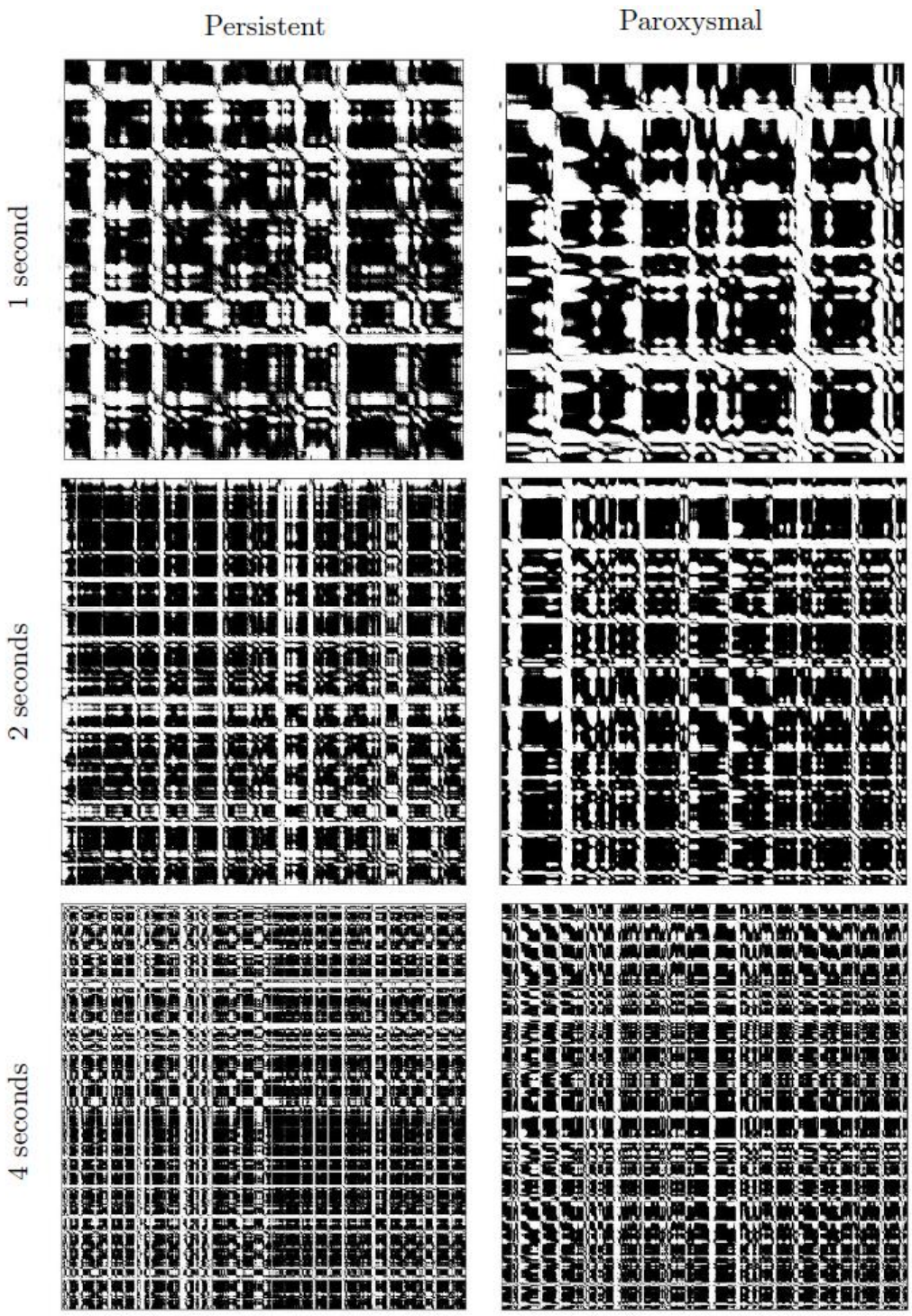

Figure 4: RPs from 1, 2 and 4 second segments measured from the left superior pulmonary vein ostia at the posterior region of the heart.

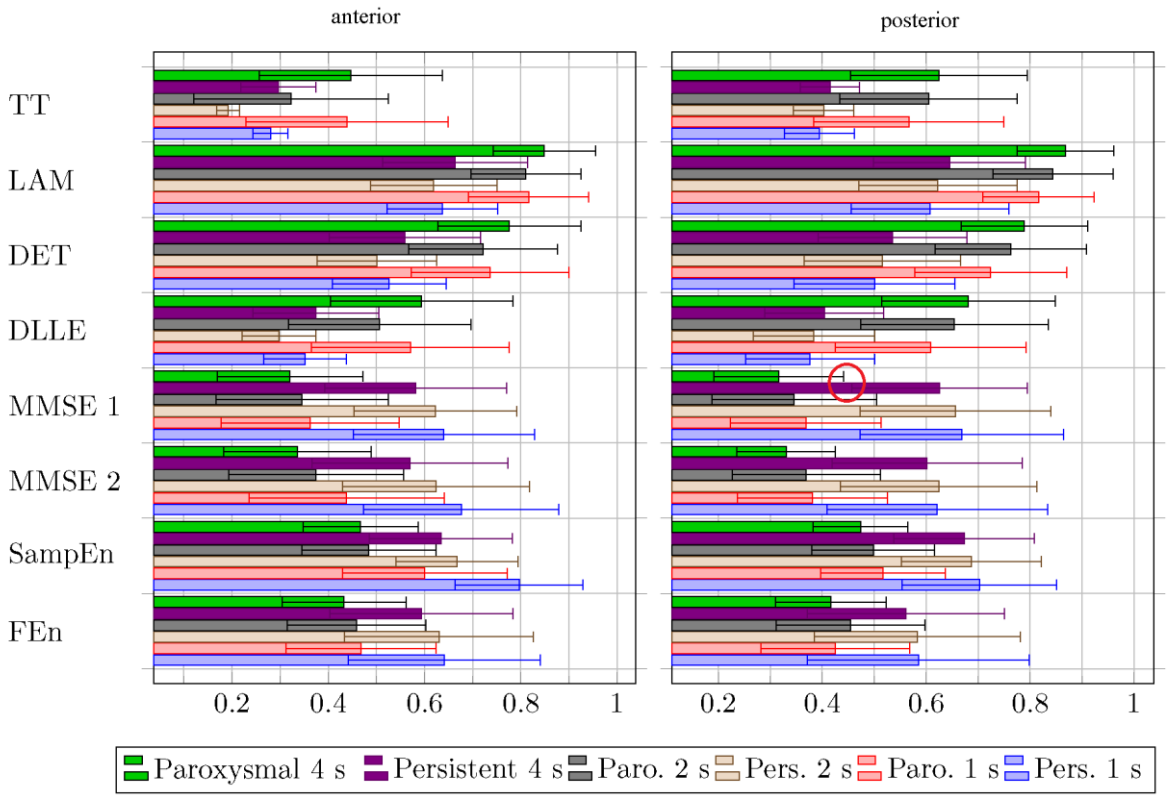

Figure 5: Mean bar plot for 1, 2 and 4 second segments of persistent as well as paroxysmal data from the LSPV. A unique range is identified with a red circle ◯.

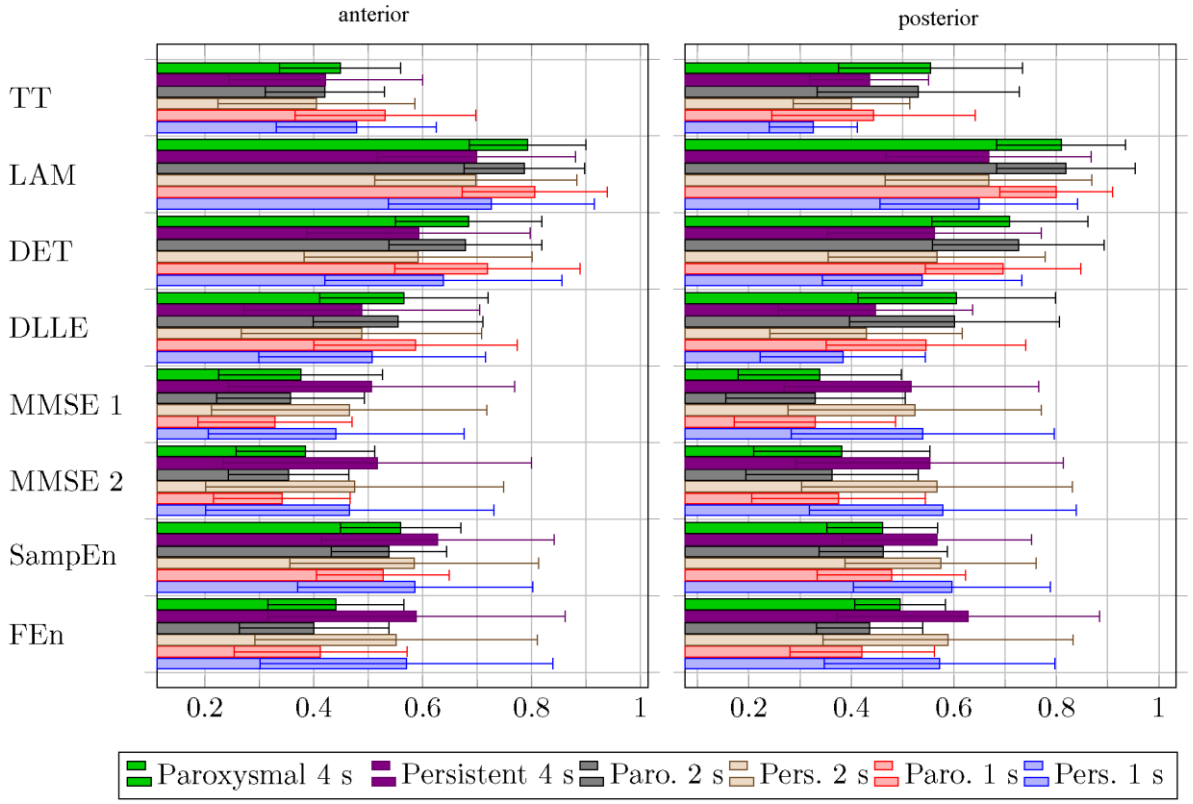

Figure 6: Mean bar plot for 1, 2 and 4 second segments of persistent as well as paroxysmal data from the LIPV.

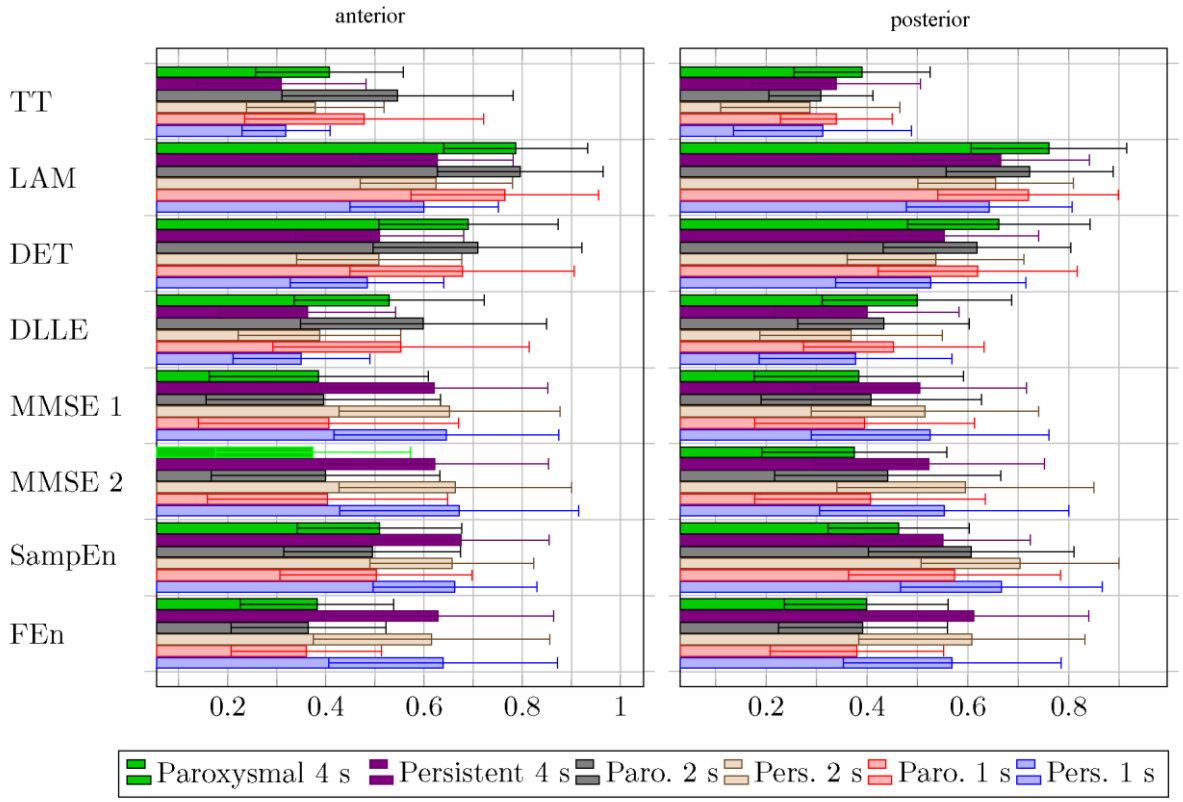

Figure 7: Mean bar plot for 1, 2 and 4 second segments of persistent as well as paroxysmal data from the RSPV.

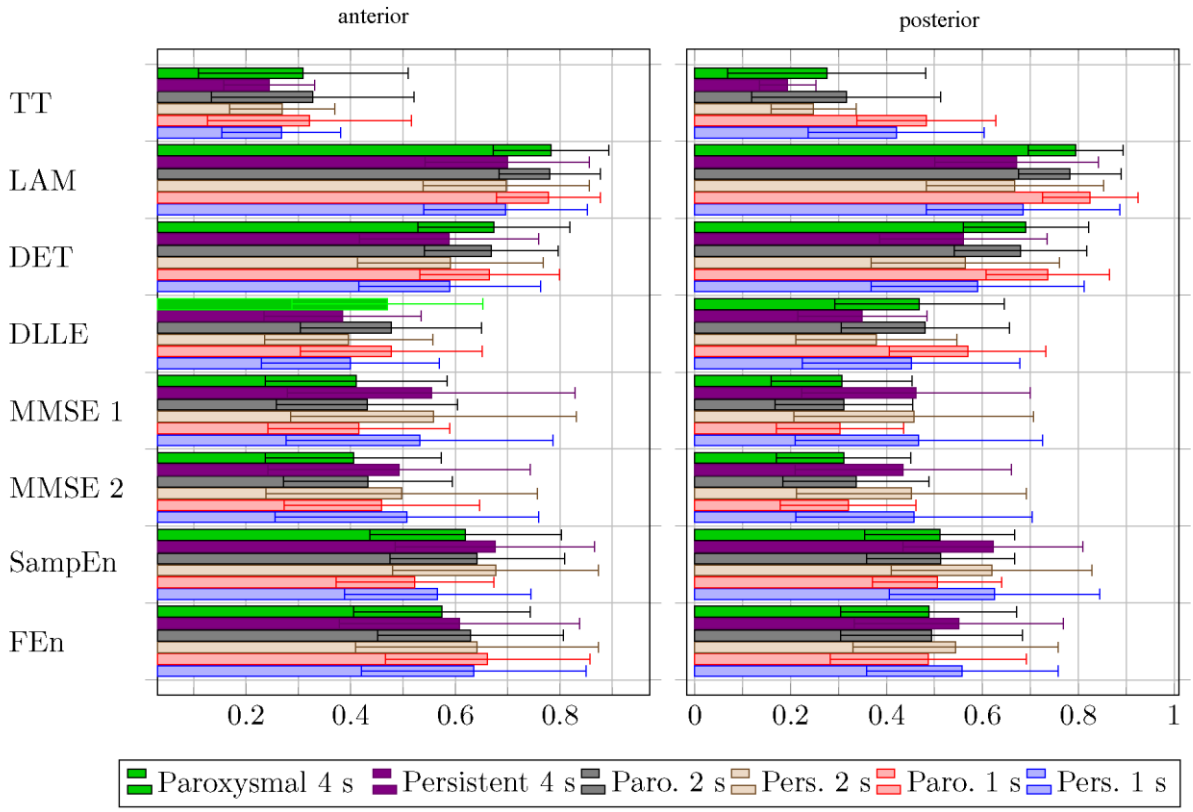

Figure 8: Mean bar plot for 1, 2 and 4 second segments of persistent as well as paroxysmal data from the RIPV.

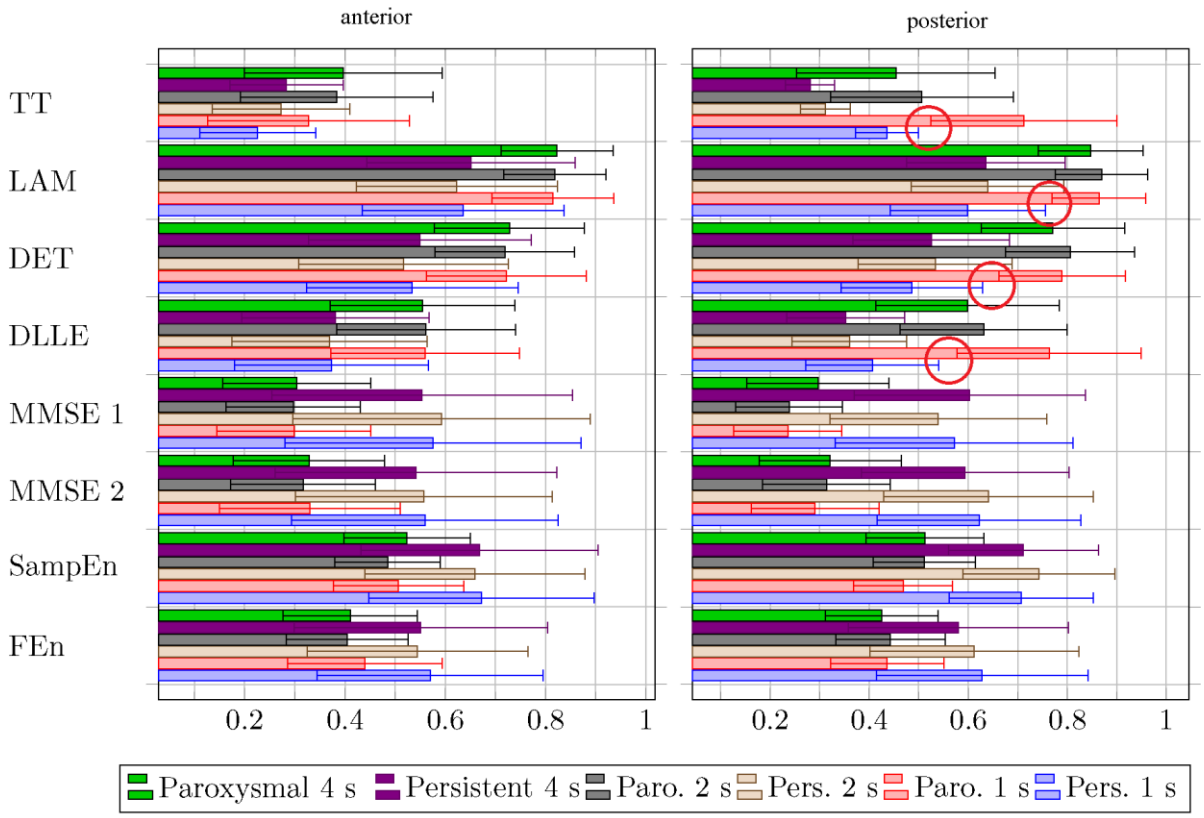

Figure 9: Mean bar plot for 1, 2 and 4 second segments of persistent as well as paroxysmal data from the POS. Unique ranges are identified with a red circle ◯.

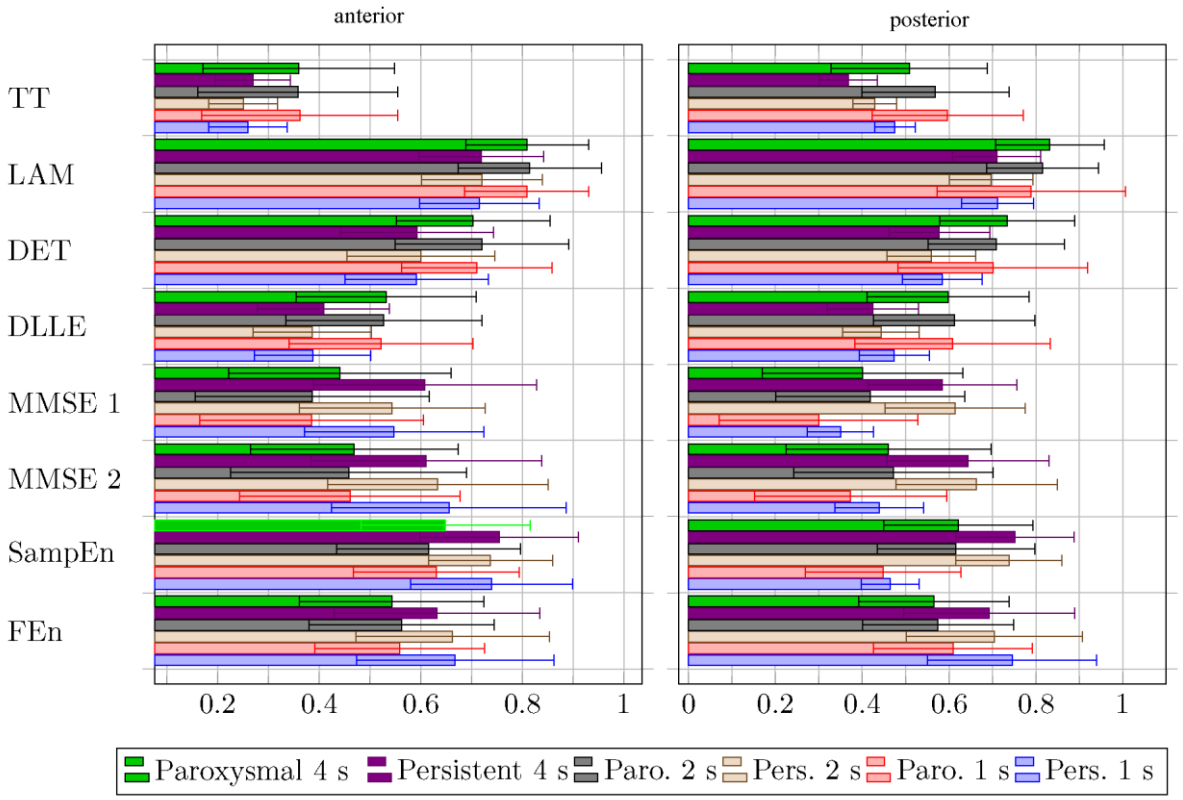

Figure 10: Mean bar plot for 1, 2 and 4 second segments of persistent as well as paroxysmal data from the ANT.

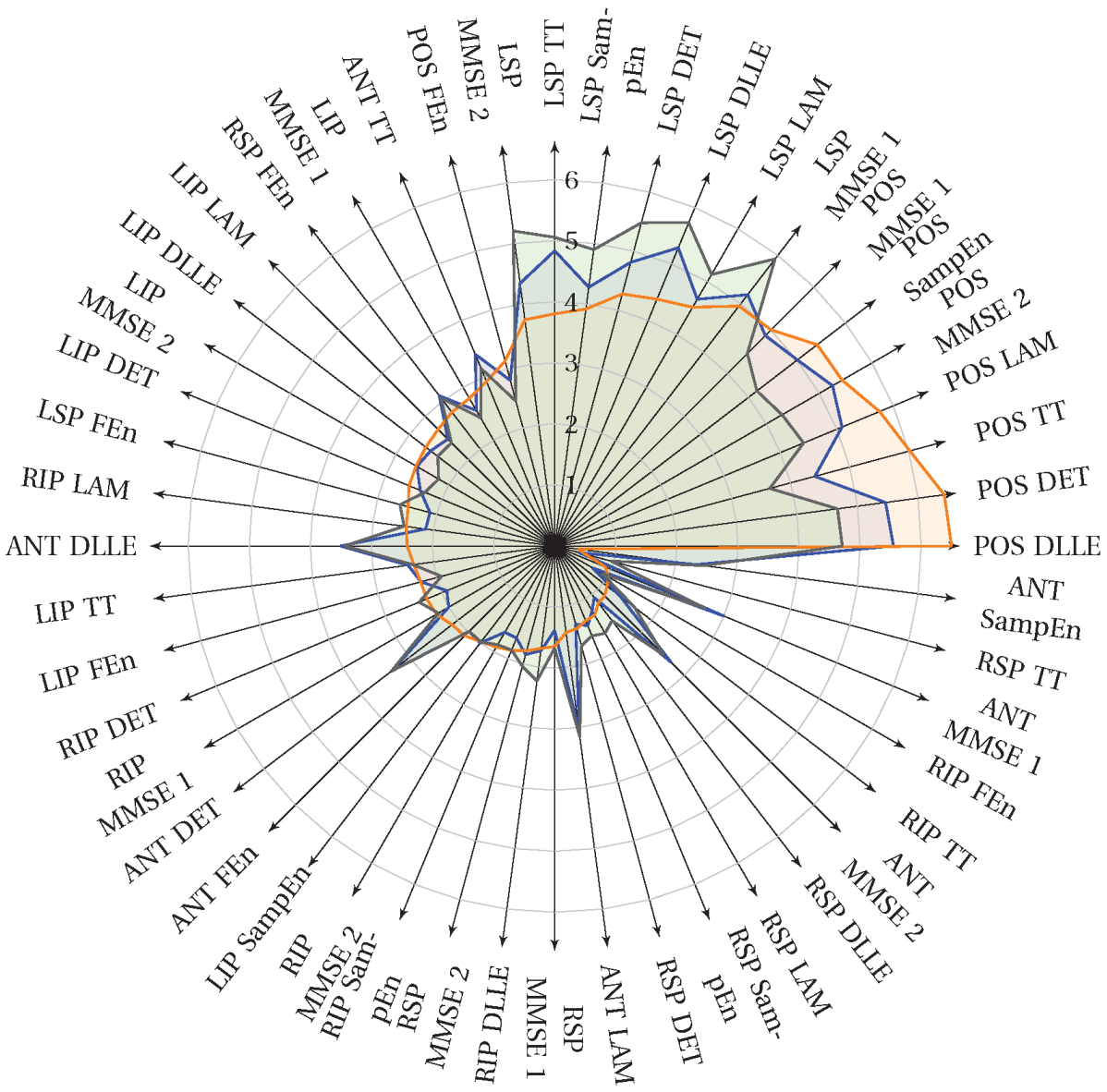

Figure 11: f-value of the RP features extracted from electrograms measured from the posterior region of the heart. The orange line represents the feature performance for 1 second signal segments. The green and blue lines represent the feature performance for 2 and 4 second signal segments respectively.

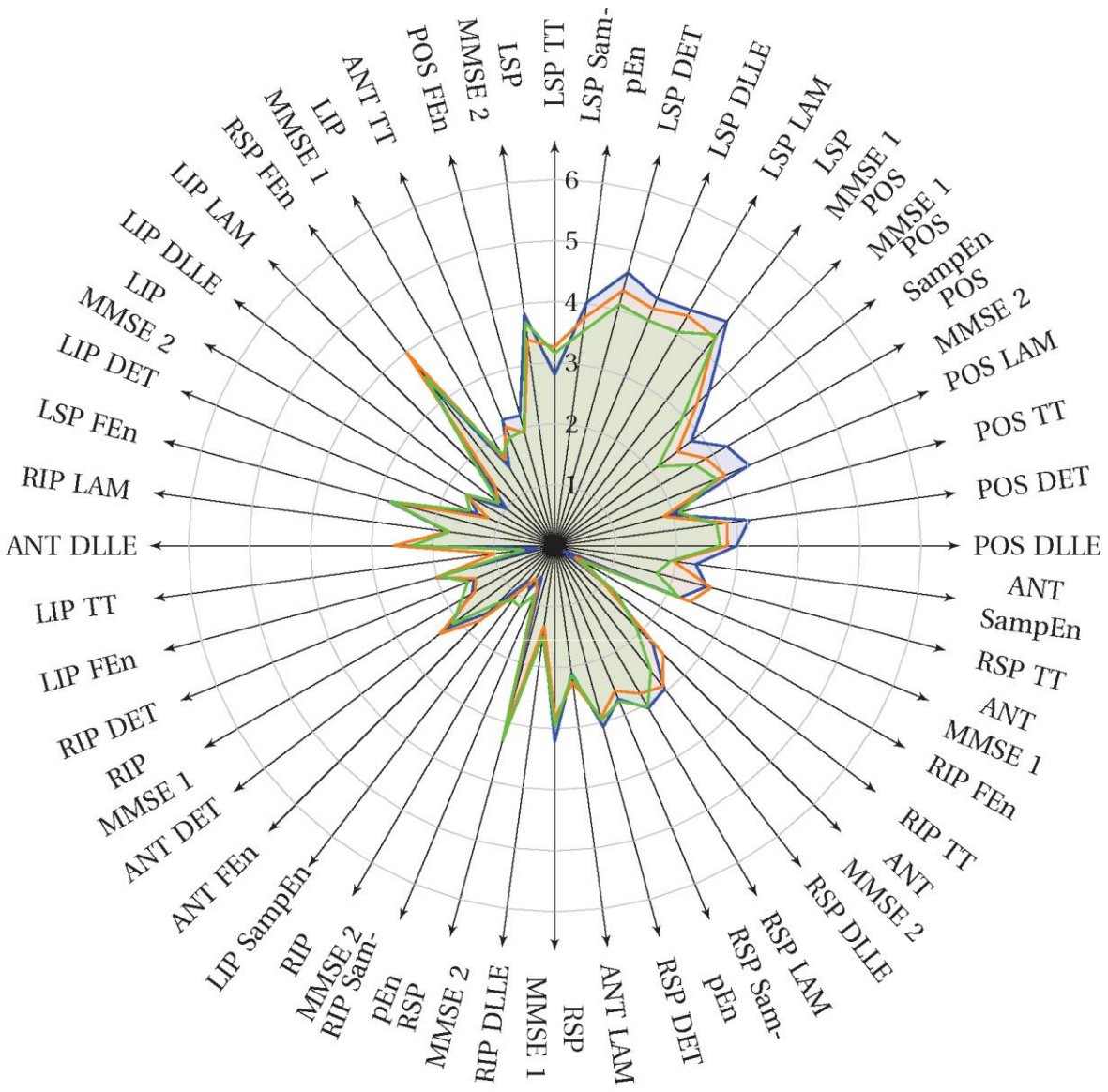

Figure 12: f-value of the RP features extracted from electrograms measured from the anterior region of the heart. The orange line represents the feature performance for 1 second signal segments. The green and blue lines represent the feature performance for 2 and 4 second signal segments respectively.